Advancements in Contact-free Respiration Monitoring using RF Pick-up coils

I. Graesslin[1], G. Mens[2], A. Guillaume[1], H. Stahl[3], P. Koken[1], P. Vernickel[1], P. Harvey[2], J. Smink[2], K. Nehrke[1], and P. Boernert[1]
[1]Philips Research Europe, Hamburg, Germany, [2]Philips Healthcare, Best, Netherlands, [3]FH Westküste, Heide, Germany

Introduction

Respiratory motion is a challenging problem in MRI, especially in the abdominal region. Advanced methods of motion detection and motion artifact reduction help to improve diagnostic image quality. SSFP sequences are commonly used in these cases. However, the use of conventional navigators [1] requires additional planning and adversely influences the steady state, which can result in image artifacts. Recently, a new approach [2, 3] was presented that makes use of the detection of changes of RF coil loading induced by the respiratory motion of the patient. This paper describes the application of such a real-time self-navigated respiration monitoring approach using dedicated RF monitoring pulses instead of using the RF excitations of the imaging sequence itself. This overcomes the problem of not being able to monitor the respiration dead times of the image acquisition, e.g. in cardiac triggered sequences. Furthermore, the problem of RF amplifier drift is analyzed, and a compensation scheme is proposed to overcome this problem.

Methods

RF coil loading is changed by patient motion, e.g. due to respiration, which can be detected during RF pulse transmission. For this purpose, the complex currents in the transmit coil are monitored via pick-up coils (PUCs). The experiments were carried out on a whole body 3T MRI system (Achieva, Philips Healthcare, The Netherlands) equipped with eight parallel RF transmit channels [4]. The system is furthermore equipped with a patient table allowing for reproducible table speed and positioning during data acquisition [5]. The complex currents of each of the eight RF transmit elements of the body coil [6] can be monitored via individual pick-up coils on each coil element. In order to decouple the respiration monitoring from the actual imaging sequence, short rectangular "monitoring pulses" of 64 µs duration were integrated into the pulse sequence as shown in Fig. 1. This approach provides more flexibility in the monitoring process than using the RF pulses of the imaging sequences themselves. Furthermore, the new approach improves the SNR of the PUC signals for very low flip angles. By using off-frequency pulses, adverse effects on the steady state are prevented. The short duration of the pulses keeps the contribution to the overall SAR very low. Using only a few RF samples makes the approach susceptible to changes in RF properties not originating from the object monitored. The forward power signal of the amplifier contains only information about the signal drift and noise caused by the amplifier but not about the object monitored. Thus, it can be used to compensate these failure impacts by subtracting it from the PUC signal. Different subtracting schemes were investigated in order to compensate for possible inter- and intra-pulse droop of the RF amplifier. The following methods of subtraction have been compared: (a) complex, (b) real part only and (c) magnitude only.

Extensive tests of motion compensation were performed by periodically moving the patient table with a saline phantom about ±15mm along z with a velocity of 50mm/s (adjustable). For a reliable verification of the displacement, a 1D-test mode was used by sampling a k0 profile in a repetitive manner while performing gradient echo imaging (TR=9ms, TE=4.4ms, α=30°, FOV=450mm). This allowed the detection of gating errors very precisely (in the order of 1mm).

Fig. 5: Image acquisition during free breathing (top), PUC-gated image (middle) and breath hold image (bottom).

Results and Discussion

4 of the 8 respiration signals from the phantom studies are shown in Fig. 2. The PUC signals are shown in blue, the corresponding drifts are shown in orange. It can be seen that amplitude and noise vary significantly depending on the position, and thus, the loading, of the individual TX coil elements. The drift of the RF amplifiers (about 0.5%) is well within the specifications and irrelevant for the imaging sequence. However, it makes reliable gating very difficult and significantly reduces the scan efficiency due to small signal variations induced by load changes. Magnitude correction of the PUC signals with the forward power measured between amplifier and circulator output result in a very efficient suppression of the drift (Fig. 3). Drift correction significantly improves the reliability of the PUC signal. To obtain more reliable signals, a model-based Kalman filter was used. A short calibration phase over a couple of respiratory cycles was found to be sufficient to calibrate a simple model [7] from the PUC signal.

The results of the 1D-projection of a resting phantom and moving phantom are shown in Fig. 4 (a) and (b), respectively. Fig. 4 (c) illustrates the result of a PUC-gated image acquisition. The monitoring GUI (Fig. 4d) shows the acquired unfiltered, but drift compensated and unfiltered PUC signal (green) at the top, Kalman filtered signal (light blue), gating window (yellow and purple) and "selection signal" (orange) (d). The processing was carried out on the real-time spectrometer with a latency of less than 20ms, which allows the use of the signal for gated image acquisition, reducing respiratory motion artifacts as shown in Fig 4 (c) and Fig. 5.

Conclusion

A flexible and very sensitive contact-free respiration monitoring approach has been demonstrated on a clinical MR system in phantom and in vivo experiments. The method has the advantage of being compatible with any imaging sequence, including ECG-triggered scans or navigators. The use of a combination of effective drift compensation and real-time Kalman filtering increases the scan efficiency and reduces the gating errors. The method represents an interesting alternative to other existing techniques.

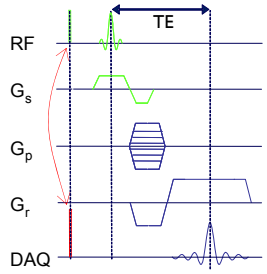

Fig. 1: A short hard RF monitoring pulse, shown in red, is sampled with the PUCs and the MR response is shown in blue.

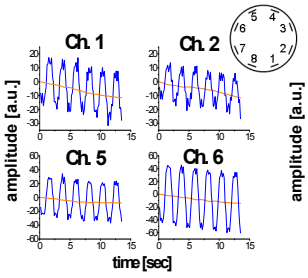

Fig. 2: Selected PUC signals (blue) and the corresponding drift (orange).

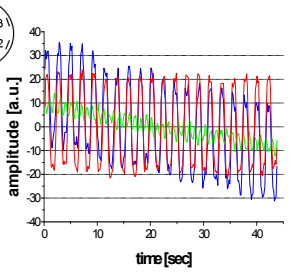

Fig. 3: Comparison uncorrected PUC signal (blue) vs. forward power (green) and corrected PUC signal (red).

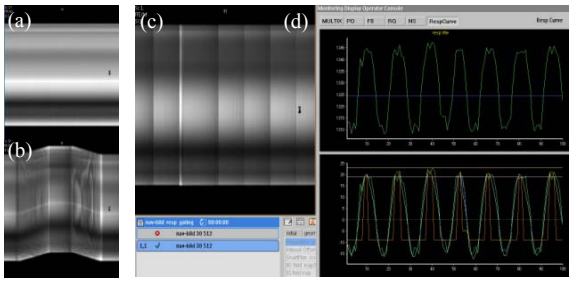

Fig. 4: 1D projection of resting phantom (a), moving phantom (b) and PUC-gated free breathing volunteer scan (c). Monitoring GUI with unfiltered PUC signal (green), Kalman filtered signal (light blue), gating window (yellow and purple) and "selection signal" (orange) (d).

References

[1] Nehrke K, et al. [1999] MRI 17:1173-81
[2] Graesslin I, et al. [2007] ISMRM 15:867
[3] Graesslin I, et al. [2009] ISMRM 17:752
[4] Graesslin I, et al. [2006] ISMRM 14:129
[5] Kruger D, et al., [2002] MRM 47(2):224-31
[6] Vernickel P, et al. [2007] MRM 58(2):381-9
[7] Spincemaille P, et al. [2008] MRM 60:158-68